Cryogenic Characterization of the High Frequency and Noise Performance of SiGe HBTs From DC to 70 GHz and Down to 2 K

S. Bonen, *Graduate Student Member, IEEE*, G. Cooke, *Graduate Student Member, IEEE*, T. Jager, A. Bharadwaj, S. Pati Tripathi, *Graduate Student Member, IEEE*, D. Céli, P. Chevalier, *Member, IEEE*, P. Schvan, *Member, IEEE*, and S. P. Voinigescu, *Fellow, IEEE*

***Abstract*— The high frequency and noise performance (T_{MIN}, NF_{MIN}, R_n, and Z_{sopt}) of SiGe heterojunction bipolar transistors (HBTs) are characterized for the first time from dc and *S*-parameter measurements up to 70 GHz and from 2 to 400 K. Significantly improved current gain ∼10 000, minimum noise temperature, T_{MIN} (<1 K below 8.5 GHz), MAG, f_T (458 GHz), and f_{MAX} (534 GHz) are observed at 2 K compared to 300 K, with no evidence of impurity deionization. It is found that the optimum noise figure current density, J_{OPT}, increases with temperature, following the crossover between shot noise and thermal noise. In contrast, the peak-f_T and peak-f_{MAX} current densities increase by more than 50% at 2 K, likely due to the higher v_{sat}. A decrease in BV_{CEO}, expected due to the higher current gain, and negative output conductance are observed in the 2–200 K range in the dc output characteristics at large currents above the peak-f_T current.**

***Index Terms*— Cryogenic temperatures, heterojunction bipolar transistor (HBT), noise, semiconductor device modeling, silicon germanium, terahertz.**

I. Introduction

THERE has been recent interest in the design of cryogenic microwave and millimeter-wave SiGe heterojunction bipolar transistor (HBT) low-noise amplifiers (LNAs) for applications in space and quantum computing [1]–[4]. To date, this work on LNAs and on the high frequency (HF) [5]–[9] and noise characterization [6] of the SiGe HBTs themselves has been conducted at temperatures above 4 K. In this letter, we report a full suite of dc, HF, and noise parameter characterization of a SiGe HBT in a production 55-nm SiGe BiCMOS process [10] from 400 K down to 2 K and derive important low-noise circuit design guidelines.

II. Measurement Methodology

All measurements were conducted on-die with a Lake Shore Cryotronics CPX-VF-LT probestation in the 2–300 K range and a Cascade Summit 9000 probestation in the 300–400 K range. The 2-K probestation is fitted with dual dc to 70-GHz differential arms, but only ground-signal-ground (GSG) probes were used for transistor characterization. The dies and the impedance standard substrate (ISS) calibration substrate were mounted on the sample holder using a silver paste with matched thermal expansion coefficient and high thermal/electrical conductivity, as illustrated in Fig. 1.

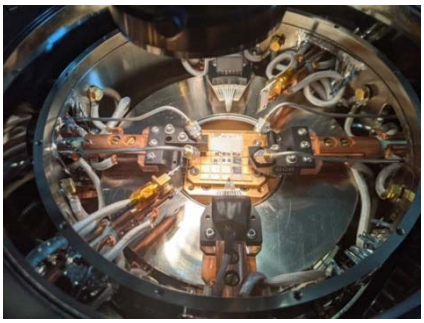

Fig. 1. Photograph of the 2-K probestation with dies bonded on sample holder, and differential dc to 70-GHz arms with GSG probes on the east and west sides.

For *S*-parameter measurements, line-reflect-reflect-match (LRRM) calibrations using the ISS substrate were conducted at 2, 20, 300, 350, and 400 K. The 20-K calibration was also used in measurements conducted at 50, 77, 200, and 250 K. The pad and interconnect parasitics of the transistor test structures were de-embedded at each temperature up to the edge of the HBT using transmission-line de-embedding with two on-die 100- and 365-μm long microstrip lines measured at each temperature. The measured *S*-parameters thus de-embedded reflect the true circuit performance of the SiGe HBT with all metal wiring up to the top metal left on the transistor. Therefore, the reported f_T and f_{MAX} values are ∼10% lower than those obtained with an open-short de-embedding method, which removes the parasitic resistance and capacitance of the interconnect on top of the transistor. The same 0.1 μm × 4.5 μm HBT with two base and two collector contacts was measured at each temperature, except at 350 and 400 K, where, due to degradation of the probe-to-pad contact resistance because of repeated landings on the same pad, an identically sized HBT from a different die was measured.

The noise parameters, R_n, T_{MIN}, and Z_{sopt}, were obtained directly from the measured dc base and collector currents, I_B and I_C, the two shot noise sources assumed to be uncorrelated below $f_T/3$, and the measured *Y*-parameters of the HBT after de-embedding, following the method in [11], without having

Manuscript received February 24, 2022; accepted March 14, 2022. Date of publication March 29, 2022; date of current version June 7, 2022. This work was supported in part by the Ontario Centres of Excellence (OCE) under Grant ECQOR5G and in part by the Ciena Corporation. *(Corresponding author: S. Bonen.)*

S. Bonen, G. Cooke, T. Jager, A. Bharadwaj, S. Pati Tripathi, and S. P. Voinigescu are with the ECE Department, University of Toronto, Toronto, M5S 3G4 ON, Canada (e-mail: shai.bonen@mail.utoronto.ca).

D. Céli and P. Chevalier are with STMicroelectronics, 38926 Crolles, France.

P. Schvan is with the Analog Design Department, Ciena Corporation, Ottawa, K2K 0L1 ON, Canada.

This article was presented at the IEEE MTT-S International Microwave Symposium (IMS 2022), Denver, CO, USA, June 19–24, 2022.

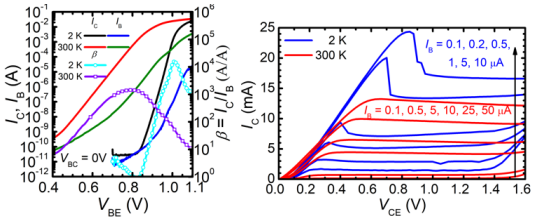

(a) (b)

Fig. 2. Measured (a) Gummel and (b) output characteristics at 2 and 300 K.

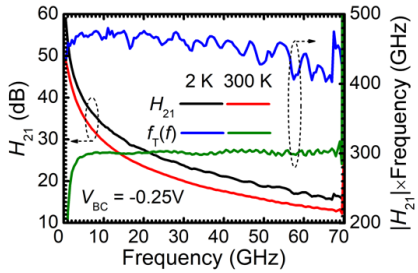

Fig. 3. Measured SiGe HBT H_{21}(f) and extrapolated $f_T(f)$ at 2 and 300 K.

to extract a small signal equivalent circuit for the HBT. It is assumed that the formulas for collector and base shot noise current power densities ($2qI_C$ and $2qI_B$) remain valid at 2 K. Equations (1) and (2), shown at the bottom of the page, describe R_n and T_{MIN}.

From (2), $F_{\mathrm{min}} = (T_{\mathrm{MIN}}/T_0 + 1)$ is derived [12]. $V_T = kT/q$, where T is the sample holder temperature and $T_0 = 290$ K. The external emitter, r_E, and the base, r_B, resistance, the dominant thermal noise sources, are extracted directly from the measured Z-parameters of the HBT. The main uncertainty at cryogenic temperatures comes from the approximation of the thermal noise power density of a resistor as 4kTR [13]. Its impact on the measured noise parameters is under investigation.

III. DC Characterization

Fig. 2 shows the measured Gummel and output characteristics at 2 and 300 K. The peak β increases from ~1000 at 300 K to 10 000 at 2 K with the $I_C(V_{\mathrm{BE}})$ and $I_B(V_{\mathrm{BE}})$ curves shifting to higher V_{BE} and exhibiting steeper slopes than at 300 K. As seen from the measured output characteristics, $\mathrm{BV_{CEO}}$ decreases at 2 K because of the increased β, while R_C improves, as evidenced by the steeper slope of the $I_C(V_{\mathrm{CE}})$ characteristics at low V_{CE}. Apart from the negative output conductance observed at the transition between the saturation and active regions at very large currents in the output characteristics, which persists up to 200 K, and whose origins are explained in [14], the HBT shows excellent behavior at 2 K with no evidence of dopant deionization.

IV. S-Parameter and Noise Characterization

The method for extrapolating f_T from the measured $H_{21}(f)$ characteristics by averaging over the 20–45 GHz range and assuming −20-dB/decade slope is illustrated in Fig. 3 at 2 and 300 K. A similar procedure is used to extrapolate f_{MAX} from $U(f)$ at each bias point. The extraction of r_E from $\mathrm{Re}\{Z_{12}(f)\}$ at large I_C and of $r_B(I_C)$ from $\mathrm{Re}\{Z_{11}(f) - Z_{12}(f)\}$ is shown in Fig. 4. Fig. 5 compiles the measured f_T and f_{MAX} versus collector current density from 2 to 400 K. The peak-f_T improves from 300 GHz at 300 K to 458 GHz at 2 K, while the peak-f_{MAX} increases from 295 GHz at 300 K to 534 GHz at 2 K. While the corresponding peak-f_T (J_{pfT}) and peak-f_{MAX} (J_{pfMAX}) current densities remain constant at 15 mA/μm^2 between 300 and 400 K, they increase by 30% and 20%, respectively, at 2 K. Since J_{pfT} is proportional to the electron saturation velocity, v_{nsat} and the doping in the

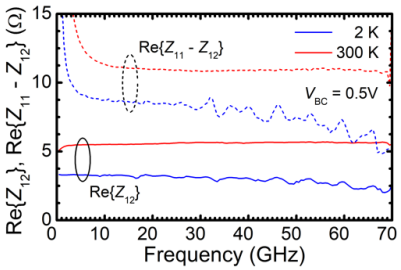

Fig. 4. Measured $\mathrm{Re}\{Z_{11}-Z_{12}\}$ and $\mathrm{Re}\{Z_{12}\}$ versus frequency in saturation for extraction of the external base and emitter resistances at 2 and 300 K.

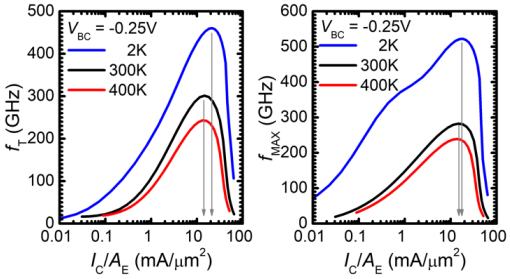

(a) (b)

Fig. 5. Measured (a) f_T and (b) f_{MAX} versus I_C/A_E and temperature at $V_{\mathrm{BC}} = -0.25$ V.

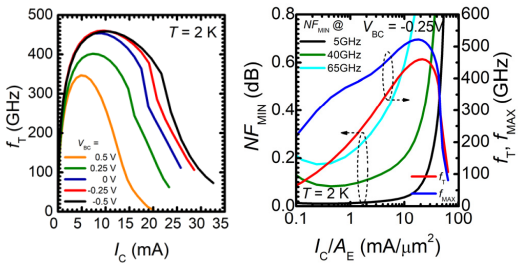

(a) (b)

Fig. 6. Measured (a) f_T versus I_C at 2 K as a function of V_{BC}. (b) f_T, f_{MAX}, and $\mathrm{NF_{MIN}}$ at 5, 40, and 65 GHz versus I_C/A_E at 2 K and $V_{\mathrm{BC}} = -0.25$ V.

$$R_n = \frac{T}{T_0}\left(r_E + r_B + \frac{I_C}{2V_T|Y_{21}|^2}\right) \tag{1}$$

$$T_{\mathrm{MIN}} = \frac{I_C T}{V_T|Y_{21}|^2}\left(\Re(Y_{11}) + \sqrt{\left(1 + \frac{2V_T|Y_{21}|^2(r_E + r_B)}{I_C}\right)\left(|Y_{11}|^2 + \frac{I_B|Y_{21}|^2}{I_C}\right) - \Im^2(Y_{11})}\right) \tag{2}$$

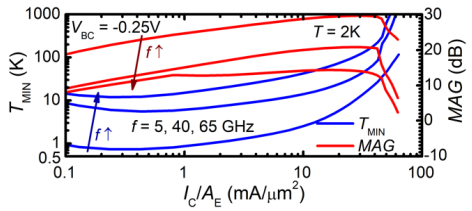

Fig. 7. Measured T_{MIN} and MAG at 5, 40, and 65 GHz versus I_C/A_E at 2 K.

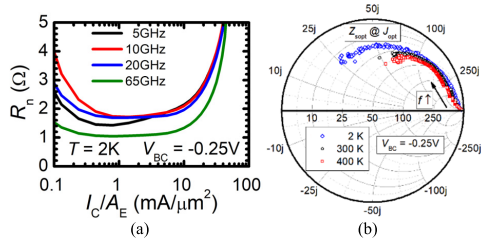

Fig. 8. Measured (a) R_n at 5, 10, 20, and 65 GHz versus I_C/A_E at 2 K for $V_{\mathrm{BC}} = -0.25$ V. (b) Z_{sopt} at J_{opt} versus frequency up to 70 GHz and temperature for $V_{\mathrm{BC}} = -0.25$ V.

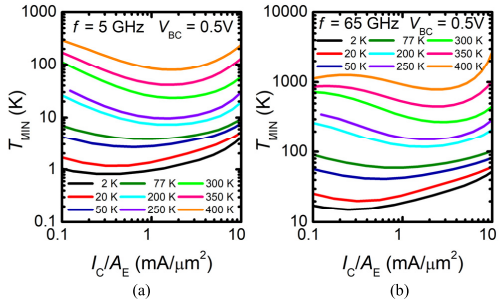

Fig. 9. Measured T_{MIN} versus I_C/A_E at (a) 5 GHz and (b) 65 GHz over temperature from 2 to 400 K at $V_{\mathrm{BC}} = 0.5$ V.

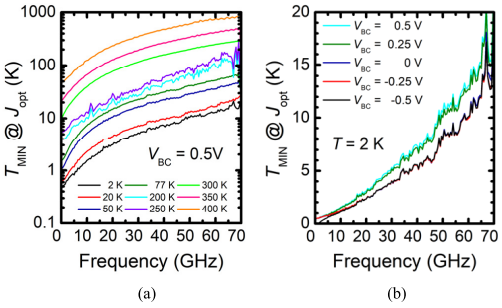

Fig. 10. Measured (a) T_{MIN} when biased at $V_{\mathrm{BC}} = 0.5$ V and J_{opt} for the given temperature and frequency, and (b) T_{MIN}, at J_{opt} versus frequency and V_{BC} at 2 K.

collector, this highlights that v_{nsat} increases at 2 K by at least 30%. Figs. 6 and 7 illustrate the 2 K measured f_T and f_{MAX} dependence on V_{BC} and I_C/A_E and of $\mathrm{NF}_{\mathrm{MIN}}$, T_{MIN}, and MAG. The f_{MAX} "hump" observed in Figs. 5(b) and 6(b) is correlated with the $I_B(I_C)$ and $r_B(I_C)$ characteristics, not shown here. Fig. 8 depicts R_n at several frequencies versus I_C/A_E, and Z_{sopt} from dc to 70 GHz, both relevant for LNA design. As shown in Fig. 9, T_{MIN} and J_{opt} increase with temperature and with frequency, while Fig. 10(a) captures the frequency dependence of T_{MIN} from 2 to 400 K and, at 2 K, for V_{BC} in the -0.5 to $+0.5$ V range, as shown in Fig. 10(b). The best T_{MIN} is lower than 1 K below 8.5 GHz, the best reported

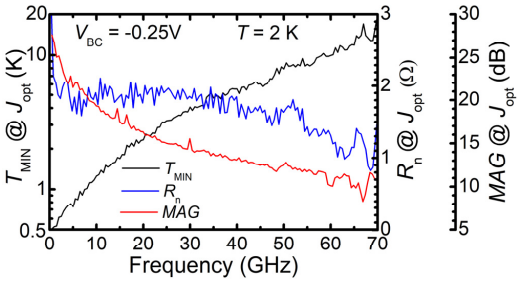

Fig. 11. Measured T_{MIN}, R_n, and MAG at J_{opt} versus frequency at 2 K when biased at $V_{\mathrm{BC}} = -0.25$ V and J_{opt} for the given frequency.

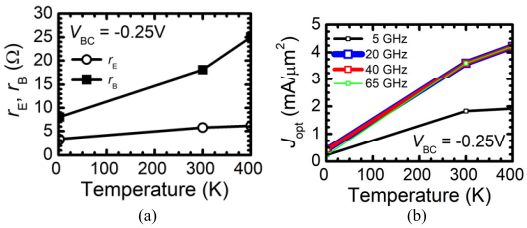

Fig. 12. Measured (a) external emitter and base resistance and (b) J_{opt} versus temperature.

for a SiGe HBT. Fig. 11 compiles the LNA-design-relevant T_{MIN}, R_n, and MAG, all at J_{opt} bias, as a function of frequency at 2 K. MAG(J_{opt}) and $T_{\mathrm{MIN}}(J_{\mathrm{opt}})$ remain higher than 10 dB and lower than 18 K, respectively, up to 70 GHz. Finally, the $\sim 10\times$ reduction in J_{opt} at 2 K from 400 K is explained by the more than linear reduction of thermal noise with temperature due to the decrease of r_E and r_B by a factor of 2 and 3, respectively, between 400 and 2 K, as shown in Fig. 12.

V. Conclusion

We have reported the on-die characterization of the HF and noise parameters of SiGe HBTs down to 2 K. The noise parameters were obtained using an established method based solely on dc and S-parameter measurements and which was validated at room temperature using direct noise parameter measurements in [11]. Without the need for dedicated noise measurements or extracting an approximate small signal equivalent circuit, this method yields very smooth noise parameters up to 70 GHz, on par with the accuracy and smoothness of the measured Y-parameters. The cryogenic noise parameters extracted using this approach still need to be verified by direct on-die noise parameter measurements with an external noise source. That remains a challenge at 2 K and is the subject of future work. Most importantly, unlike g_m, f_T, and f_{MAX}, which saturate below 70 K (not shown), T_{MIN} continues to decrease down to at least 2 K, with a record value of 0.62 K at 5 GHz. Since J_{opt} also decreases by approximately a factor of 10 between 300 and 2 K, low-noise amplifier design requires a dedicated HiCUM model, extracted at 2 K. This remains a challenging topic to be addressed in future research.

Acknowledgment

The authors would like to acknowledge STMicroelectronics, Crolles, France for 55-nm SiGe BiCMOS die fabrication and donation. They would also like to acknowledge Keysight for testing support, CMC for CAD tools, and Jaro Pristupa for CAD support.

REFERENCES

[1] F. Arute *et al.*, "Quantum supremacy using a programmable superconducting processor," *Nature*, vol. 574, no. 7779, pp. 505–510, 2019.

[2] Z. Zou *et al.*, "A frequency and bandwidth reconfigurable 3–6 GHz cryogenic SiGe BiCMOS LNA with power consumption of $\leq$2.9 mW," in *IEEE MTT-S Int. Microw. Symp. Dig.*, Jun. 2021, pp. 653–656.

[3] W. Wong, M. Hosseini, H. Rücker, and J. C. Bardin, "A 1 mW cryogenic LNA exploiting optimized SiGe HBTs to achieve an average noise temperature of 3.2 k from 4–8 GHz," in *IEEE MTT-S Int. Microw. Symp. Dig.*, Jun. 2020, pp. 181–184.

[4] M. Varonen *et al.*, "Cryogenic W-band SiGe BiCMOS low-noise amplifier," in *IEEE MTT-S Int. Microw. Symp. Dig.*, Aug. 2020, pp. 185–656.

[5] H. Rucker, J. Korn, and J. Schmidt, "Operation of SiGe HBTs at cryogenic temperatures," in *Proc. IEEE Bipolar/BiCMOS Circuits Technol. Meeting (BCTM)*, Oct. 2017, pp. 17–20.

[6] S. Pruvost, "Microwave and noise performance of SiGe BiCMOS HBT under cryogenic temperatures," *IEEE Electron Device Lett.*, vol. 26, no. 2, 105-108, Feb. 2005.

[7] R. Krithivasan *et al.*, "Half-terahertz operation of SiGe HBTs," *IEEE Electron Device Lett.*, vol. 27, no. 7, pp. 567–569, Jul. 2006.

[8] P. Chevalier, N. Zerounian, B. Barbalat, F. Aniel, and A. Chantre, "On the use of cryogenic measurements to investigate the potential of Si/SiGe: C HBTs for terahertz operation," in *Proc. IEEE Bipolar/BiCMOS Circuits Technol. Meeting*, Sep. 2007, pp. 26–29.

[9] N. Zerounian, F. Aniel, B. Barbalat, P. Chevalier, and A. Chantre, "500 GHz cutoff frequency SiGe HBTs," *Electron. Lett.*, vol. 43, no. 14, p. 774, 2007.

[10] P. Chevalier *et al.*, "A 55 nm triple gate oxide 9 metal layers SiGe BiCMOS technology featuring 320 GHz fT/370 GHz fMAX HBT and high-Q millimeter-wave passives," in *IEDM Tech. Dig.*, Dec. 2014, pp. 77–79.

[11] S. P. Voinigescu *et al.*, "A scalable high-frequency noise model for bipolar transistors with application to optimal transistor sizing for low-noise amplifier design," *IEEE J. Solid-State Circuits*, vol. 32, no. 9, pp. 1430–1439, Sep. 1997.

[12] H. A. Haus *et al.*, "Representation of noise in linear twoports," *Proc. IRE*, vol. 48, no. 1, pp. 69–74, Jan. 1960.

[13] A. Kerr and J. Randa, "Thermal noise and noise measurements—A 2010 update," *IEEE Microw. Mag.*, vol. 11, no. 6, pp. 40–52, Oct. 2010.

[14] J. Yuan *et al.*, "An investigation of negative differential resistance and novel collector–current kink effects in SiGe HBTs operating at cryogenic temperatures," *IEEE Trans. Electron Devices*, vol. 54, no. 3, pp. 504–516, Mar. 2007.

Important Notice